

Nonlinear Regge trajectories and glueballs

M. M. Brisudova*

*Nuclear Theory Center, Indiana University, 2401 Milo B. Sampson Lane, Bloomington, Indiana 47408[†]*L. Burakovsky[‡] and T. Goldman[§]*Theoretical Division, MS B283, Los Alamos National Laboratory, Los Alamos, New Mexico 87545*A. Szczepaniak^{||}*Physics Department and Nuclear Theory Center, Indiana University, 2401 Milo B. Sampson Lane, Bloomington, Indiana 47408*

(Received 5 March 2003; published 22 May 2003)

We apply a phenomenological approach based on nonlinear Regge trajectories to glueball states. The parameters, i.e., the intercept and threshold, or trajectory termination point beyond which no bound states should exist, are determined from Pomeron (scattering) data. The systematic errors inherent to the approach are discussed. We then predict the masses of the glueballs on the tensor trajectory. For comparison, the approach is applied to available quenched lattice data. We find a discrepancy between the lattice-based thresholds and the Pomeron threshold that we extract from data.

DOI: 10.1103/PhysRevD.67.094016

PACS number(s): 12.39.Ki, 12.40.Nn, 12.40.Yx, 12.90.+b

I. INTRODUCTION

In a previous work [1] we presented theoretical arguments and strong phenomenological evidence that Regge trajectories of ordinary quark-antiquark mesons are essentially nonlinear and can be well approximated, for all practical purposes, by a specific function, the so-called square-root form. With a few additional assumptions intended to reduce the number of independent parameters, and, when possible, tested for self-consistency, we obtained a remarkable agreement with *both* the bound (resonant) state ($t > 0$) and scattering ($t < 0$) data. What makes this success even more impressive is the fact that the input parameters, with the exception of one, were determined by the masses of only a few lowest-lying bound states.

The theoretical motivation for our previous study was the view that the properties of the gluon field, e.g., the flux tube, change with the increasing size of the hadron. At long enough distances, a linear potential is simply a wrong approximation to the interaction of meson constituents. Therefore, Regge trajectories cannot be asymptotically linear [2] in t , even if they appear to be so over a limited range of t . In searching for a more practical approximation, we studied nonlinear Regge trajectories corresponding to dual amplitudes with Mandelstam analyticity (DAMA) [3] in a simplified situation, that is, toy models which, nevertheless, maintain a resemblance to QCD [1,4,5]. After a thorough investigation, we argued that (i) DAMA amplitudes can be expected to fit spectra, (ii) nonlinearity arises due to the color

screening of the flux tube, and, thus, (iii) one can expect the same qualitative behavior of the trajectories regardless of the quantum number of the quark-antiquark meson.

In this paper we attempt to go beyond ordinary quark-antiquark mesons to trajectories for glueballs. However, it is not *a priori* clear that non- $q\bar{q}$ mesons such as glueballs or hybrids can be satisfactorily described by the same form of Regge trajectories as are ordinary mesons. Even though the nonlinearity of Regge trajectories is due to color screening, which is not exclusive to $q\bar{q}$ mesons, the behavior of glue in exotic systems can be different. In particular, in the case of glueballs there have been contradictory opinions about the basic nature of these states, ranging from solitonic through loops of glue to glue strings. The latest lattice QCD results indicate that the loops-of-glue picture does not agree with the lattice spectra to the extent that the bag model does, thus supporting a constituentlike picture for gluons (in addition to quarks) [6]. (However, it should be kept in mind that the flux tube model is, by definition, a very simple model with a big symmetry group and so cannot be used to make detailed predictions for the spectrum; the flux-tubelike distribution of the fields should be measured instead.) The same authors view hybrids as states where a quark and an antiquark are subject to a potential corresponding, roughly speaking, to an excited flux tube. They generate a plethora of these potentials in quenched QCD. Obviously, in unquenched QCD the picture can be drastically different. It is, unfortunately, challenging and difficult at present to capture the physics of string breaking accurately with lattice methods [6]. Here we focus on pure gluonic states and only comment on the prospect of extending our analysis to hybrid mesons in the conclusion.

Encouraged by the lattice QCD analysis of Ref. [6], we apply the same phenomenological approach that worked so remarkably well for ordinary mesons to the Pomeron trajectory. In a departure from our previous calculations, we analyze scattering data to fit parameters of the square-root Regge trajectory. Naturally, in this case the extracted value

*Electronic address: martina_brisudova@mentor.com

[†]On leave from: Physics Institute, Slovak Acad. Sci., Dúbravská cesta 9, 842 28 Bratislava, Slovakia; present address: Mentor Graphics Corporation, 880 Ridder Park Drive, San Jose, CA 95131.[‡]Electronic address: burakov@lanl.gov[§]Electronic address: tgoldman@lanl.gov^{||}Electronic address: aszczepa@indiana.edu

of the threshold, or termination point of the real part of the trajectory, is subject to a large uncertainty. To reduce the uncertainty, we add to our data set the mass of the lowest-lying tensor glueball determined in Ref. [6].

[There are a number of other lattice QCD determinations of this mass, see e.g. Refs. [7], but the rms variation of the values reported is only about 1%, which is considerably smaller than the uncertainties in the individual determinations. Hence, choosing one specific case has a negligible effect on our results compared to the overall (statistical and systematic) uncertainties below and avoids a perhaps unrealistic reduction of the total uncertainty.]

With this addition, the uncertainties in the trajectory parameters are significantly reduced while the values are little affected. We take the value of the threshold as an indication of a maximum mass beyond which no glueball states exist, bearing in mind that we are unable to prove at present that the square-root form will be as comparably efficient in describing glueballs as it was for ordinary mesons.

We should also note that the threshold we find here is larger than what is inferred from trajectories fitted to quenched lattice QCD glueball mass states. Whether this is due to the difference between quenched and unquenched QCD, or the functional forms used for the trajectories, remains unknown.

The choice of a specific trajectory within the allowed range of DAMA trajectories introduces an unknown systematic error. In case of ordinary mesons, our results justified the assumptions *a posteriori*. Due to insufficient data, this is not possible when dealing with pure glue trajectories. To estimate the systematic errors, we repeat the fit with the other limiting form of DAMA trajectories, the so-called logarithmic form. We take the difference between the thresholds obtained as indicative of the systematic errors.

While the Pomeron trajectory is the only glueball trajectory for which unambiguous data exist, it may be, unfortunately, affected by the gluon condensate. In the absence of experimental glue bound-state data, we use glueball masses from lattice QCD to determine the thresholds of other, less peculiar trajectories, bearing in mind that the masses are subject to the quenched approximation.

This paper is organized as follows. Section II starts with a brief introduction to the DAMA trajectories, followed by our fits to Pomeron data. We compare the fits for the two limiting forms of trajectories, and discuss the physical meaning of the results. Section III is devoted to glueball spectroscopy. We conclude with a comment on possible future applications.

II. DAMA TRAJECTORIES AND FITS TO DATA

The class of dual models called dual amplitudes with Mandelstam analyticity (DAMA) [3] is a generalization of Veneziano amplitudes [8] to the most general form consistent with Mandelstam analyticity. [DAMA has the Veneziano limit $\alpha(t) \sim t$, but the transition to this limit occurs discontinuously [9].]

A meson trajectory $\alpha_{j\bar{i}}(t)$, can be parametrized on the entire physical sheet in the following form:

$$\alpha_{j\bar{i}}(t) = \alpha_{j\bar{i}}(0) + \gamma_\nu [T_{j\bar{i}}^\nu - (T_{j\bar{i}} - t)^\nu], \quad 0 \leq \nu \leq \frac{1}{2} \quad (1)$$

(up to a power of a logarithm), assuming that $\alpha_{j\bar{i}}(t)$ is an analytic function having a physical cut from some value t_0 to ∞ , it is polynomially bounded on the entire physical sheet, and there exists a finite limit of the trajectory phase as $|t| \rightarrow \infty$ [10]. The subscripts i, j indicate dependence of the parameters on the flavor content of the meson within a meson multiplet. In this paper we drop the subscripts for simplicity.

The parameter γ_ν is the universal asymptotic slope for nonlinear trajectories [11],

$$\alpha(t) \sim -\gamma_\nu (-t)^\nu, \quad |t| \rightarrow \infty;$$

both γ_ν and the exponent ν are independent of quantum numbers. In order for the slope to be positive at small t , $\gamma_\nu > 0$. The intercept $\alpha_{j\bar{i}}(0)$ varies for different trajectories, and in accordance with the Froissart bound should satisfy $\alpha_{j\bar{i}}(0) \leq 1$. In reality, however, there is an exception — the intercept of the Pomeron trajectory is observed to be slightly larger than 1. The parameter $T_{j\bar{i}}$ is often called the trajectory threshold.

Note that for $|t| \ll T$, Eq. (1) reduces to a (quasi)linear form:

$$\alpha_{j\bar{i}}(t) = \alpha_{j\bar{i}}(0) + \nu \gamma T_{j\bar{i}}^{\nu-1} t = \alpha_{j\bar{i}}(0) + \alpha'_{j\bar{i}}(0) t. \quad (2)$$

The value of ν is restricted to lie between 0 and 1/2, in accordance with Ref. [9]. The value $\nu=0$ should be understood as a limit $\nu \rightarrow 0$, $\gamma_\nu \nu$ fixed. In this limit, the difference of fractional powers reduces to a logarithm, viz.,

$$\alpha(t) = \alpha(0) - \gamma_{\log} \log \left(1 - \frac{t}{T_{\log}} \right), \quad \gamma_{\log} \equiv \lim_{\nu \rightarrow 0} \gamma_\nu \nu. \quad (3)$$

Unlike a trajectory with any value of $\nu \neq 0$, the real part of the “logarithmic” trajectory does not freeze-out when t reaches T . The real part continues to grow; the only change for $t > T$ is that the trajectory acquires a constant imaginary part.

The upper bound on ν gives the so-called “square-root” trajectory, viz.

$$\alpha(t) = \alpha(0) + \gamma_{1/2} [\sqrt{T} - \sqrt{T-t}]. \quad (4)$$

When t reaches T , the real part of the “square-root” trajectory stops growing, and there are no states with a higher angular momentum than $l_{max} = [\alpha(T)]$. For this reason, the parameter T is also called the trajectory termination point. This is true for any value of $\nu \neq 0$.

A. Fit with the square-root form

In Ref. [1] we used only the square-root form of Eq. (4) for spectroscopy purposes. We determined the value of $\gamma_{1/2}$ from the ρ trajectory, and then it was taken as universal for all other meson trajectories. Our calculation is in excellent agreement with various data, not only spectroscopic but scattering as well, and is self-consistent, justifying the assumption

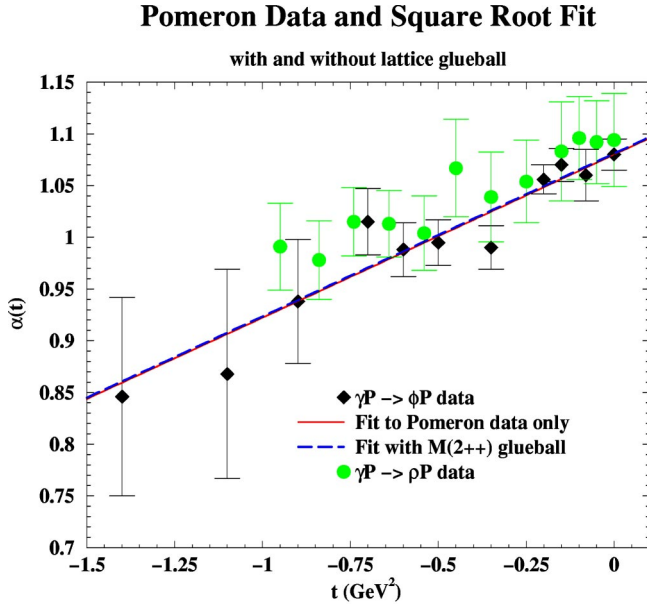


FIG. 1. Pomeron data together with our best fits of the square-root form: The dashed line fit includes the averaged mass $M(2^{++})$ as a data point; for the solid line fit only the scattering data were used.

tions *a posteriori*. This leads us to believe that the extracted value of $\gamma_{1/2}$ is reliable, and that the square-root form is close to the true functional form of meson trajectories.

Since γ_ν must be a constant *independent* of the flavor content or quantum numbers of the meson, we apply the same value,

$$\gamma_{1/2} = 3.65 \pm 0.05 \text{ GeV}^{-1}, \quad (5)$$

to the data for the Pomeron.

With the value of the universal asymptotic slope fixed, we can now fit the Pomeron scattering data to find the remaining parameter of the Pomeron trajectory, $T_{1/2}$. Of the two data sets [12] shown in Fig. 1, we use only $\gamma p \rightarrow \phi p$ since at ZEUS energies it is devoid of significant contributions from exchanges other than the Pomeron. For comparison, we show both sets of data. Note that the data points corresponding to $\gamma p \rightarrow \rho^0 p$ are consistently above the $\gamma p \rightarrow \phi p$ as expected due to contributions from additional exchanges.

In Fig. 1, the solid line shows our best fit of the square-root form, Eq. (4):

$$\alpha_{1/2}(0) = 1.08 \pm 0.01, \quad (6)$$

$$\sqrt{T_{1/2}} = 11.56 \pm 2.08 \text{ GeV},$$

$$\chi^2/\text{d.o.f.} = 6.07/9. \quad (7)$$

The relatively large, 18% error on the fitted threshold is caused in part by the data uncertainties, and in part by the fact that all data points are concentrated in a small region of t near zero; consequently, $|t| \ll T$. The fit is essentially dominated by the first term in the Taylor expansion of Eq. (4):

$$\alpha_{1/2}(t) = \alpha(0) + \frac{\gamma_{1/2}}{2\sqrt{T_{1/2}}} t \quad (8)$$

$$= 1.08 + 0.1578 [\text{GeV}^{-2}] t. \quad (9)$$

In order to determine the threshold with better accuracy, additional data are needed. We use the mass of the lowest-lying tensor glueball from Ref. [6], $M(2^{++}) = 2.40 \pm 0.13 \text{ GeV}$. With this additional data point, the error on the extracted threshold is reduced by factor of 2, while the χ^2 of the fit remains comparably small and the fitted parameter values are essentially unchanged (see Fig. 1). In this way we obtain

$$\alpha_{1/2}(0) = 1.081 \pm 0.007, \quad (10)$$

$$\sqrt{T_{1/2}} = 11.57 \pm 1.1 \text{ GeV},$$

$$\chi^2/\text{d.o.f.} = 6.07/10. \quad (11)$$

We note that the $\chi^2/\text{d.o.f.}$ in both cases is smaller than one would expect on general grounds. This is similar to the case observed in Ref. [13] for other trajectories, presumably for similar reasons.

B. Fit with the logarithmic form

Even though the logarithmic trajectory, Eq. (3), itself is not realistic, since its real part grows without bound [in contrast to any other trajectory of our nonlinear form, Eq. (2), with $\nu \neq 0$], it is useful to study because the true trajectory can lie anywhere between the two limiting forms. In addition to this reason, comparison of the fits with the two limiting forms can, to some extent, illuminate the issue of systematics. There is undoubtedly a systematic error associated with the choice of DAMA trajectories as the class of trajectories within which the true trajectory lies, and this we cannot estimate. There is an additional systematic error arising from the specific choice of $\nu = 1/2$ within the model and from the way we determine the parameters of the trajectories. It is this second uncertainty that we address in this section.

To fit the data with a logarithmic form, we first need to determine the value of γ_{\log} . In complete analogy with our calculation utilizing the square-root form, the value of γ_{\log} is determined from the ρ trajectory. We find

$$\gamma_{\log} = 8.00 \pm 0.34. \quad (12)$$

Note that γ_{\log} is dimensionless.

Our best fit of the logarithmic form, Eq. (3), to the scattering Pomeron data,

$$\alpha_{\log}(0) = 1.08 \pm 0.01, \quad (13)$$

$$\sqrt{T_{\log}} = 7.09 \pm 0.64 \text{ GeV},$$

$$\chi^2/\text{d.o.f.} = 6.07/9 \quad (14)$$

is shown in Fig. 2. Also in Fig. 2, we show the fit to the scattering data plus mass of the tensor glueball, yielding

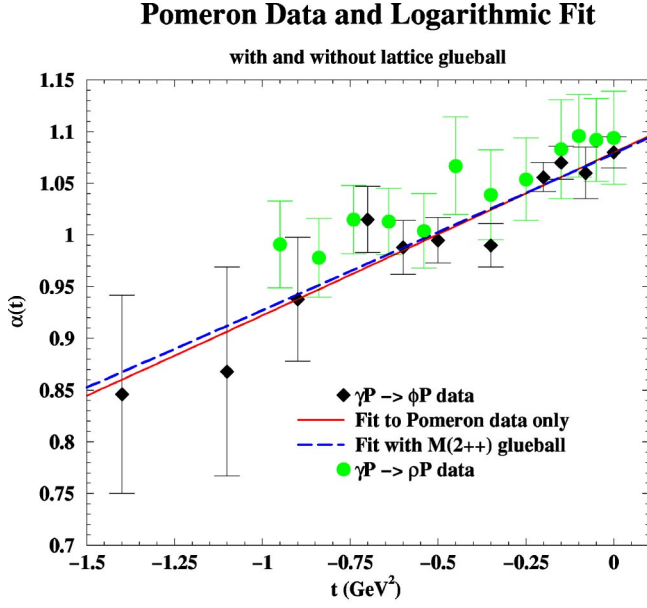


FIG. 2. Pomeron data together with our best fits of the logarithmic form: The dashed line fit includes the averaged mass $M(2^{++})$ as a data point; for the solid line fit only the scattering data were used.

$$\alpha_{\log}(0) = 1.079 \pm 0.007,$$

$$\sqrt{T_{\log}} = 7.23 \pm 0.34 \text{ GeV}, \quad (15)$$

$$\chi^2/\text{d.o.f.} = 6.12/10. \quad (16)$$

The addition of the bound state data point leads to a 2% increase in $\sqrt{T_{\log}}$ and almost a factor of 2 reduction in its error. Recall that, for the square-root form, the threshold remains almost the same (less than 0.1% change).

Again, not surprisingly, the fit is dominated by the linear term

$$\alpha_{\log}(t) = \alpha(0) + \frac{\gamma_{\log}}{T_{\log}} t \quad (17)$$

$$= 1.08 + 0.1590 [\text{GeV}^{-2}]t. \quad (18)$$

C. Estimate of systematic error

The linear term dominance in all of our fits implies that the thresholds of the square root and logarithmic trajectories, extracted from Pomeron data, are simply related. The relative size of the threshold for the two limiting forms follows directly from comparison of the two linearized trajectories, Eq. (8) and Eq. (17):

$$T_{\log} = 2 \frac{\gamma_{\log}}{\gamma_{1/2}} \sqrt{T_{1/2}}. \quad (19)$$

The ratio of $\gamma_{\log}/\gamma_{1/2}$ is, in our calculation, fixed by the ρ trajectory data used as input. To find the three parameters of the ρ trajectory (its intercept, threshold, and the universal parameter γ_{ν} for any chosen ν), we restrict the trajectory to

pass through the three experimentally well established points, specifically the intercept, and the mass and spin of the ρ and the ρ_3 .

The straight line that crosses ρ and ρ_3 leads to an intercept smaller than the observed value. This means that the linear form is insufficient [1]. By an *a posteriori* comparison of the DAMA trajectory to its truncated Taylor series, one can see that the fit is basically dominated by terms up to $O(t^2)$, viz.

$$\tilde{\alpha}_{1/2}(t) \approx \tilde{\alpha}(0) + \frac{\gamma_{1/2}}{2\tilde{T}_{1/2}} t + \frac{\gamma_{1/2}}{8\tilde{T}_{1/2}^2} t^2, \quad (20)$$

$$\tilde{\alpha}_{\log}(t) \approx \tilde{\alpha}(0) + \frac{\gamma_{\log}}{\tilde{T}_{\log}} t + \frac{\gamma_{\log}}{2\tilde{T}_{\log}^2} t^2. \quad (21)$$

(We use the tilde to distinguish the ρ trajectory from the Pomeron trajectory discussed so far.) For example, the square-root trajectory evaluated at the mass of the ρ_3 differs from its Taylor series, Eq. (20), by less than 0.5%.

Setting the Taylor series coefficients in Eqs. (20) and (21) equal, we obtain

$$\tilde{T}_{\log} \approx 2\tilde{T}_{1/2}, \quad (22)$$

$$\gamma_{\log} \approx \gamma_{1/2} \sqrt{\tilde{T}_{1/2}}. \quad (23)$$

This leads to the following relation for the Pomeron thresholds:

$$T_{\log} \approx 2 \sqrt{\tilde{T}_{1/2}} \sqrt{T_{1/2}}. \quad (24)$$

The numerical values we find are in a good agreement with these relations.

Is there anything deep about these relations? Note that Eqs. (22) and (23) are a direct consequence of the fit being dominated by up to quadratic terms in t and our requirement that the trajectory pass *exactly* through the three input points. Thus, Eq. (23) cannot hold for a universal γ unless all thresholds are identical. Alternatively, the three-point restriction is too strong and/or only one specific value of ν can be correct.

D. Understanding the systematic error in terms of toy models

To understand this issue further, we turn to our toy models [1]. Within the framework of our generalized string model, it is possible to reconstruct the potential from a Regge trajectory [1,4]. Earlier we found that potentials corresponding to the square-root and to the logarithmic trajectories, respectively, are very close, when normalized to the same asymptotic value. Furthermore, they are also very close to a potential found from a fit to lattice data [14] that we used in another toy model, which consists, basically, of a leading order Born-Oppenheimer (LOBO) approximation for a system of a very heavy quark and antiquark. In that toy model, we found that the spectrum could be equally well fitted by both limiting forms of the Regge trajectories, with nearly the same thresholds [1].

The difference between the toy model study and the situation at hand is the following: In the toy model we *fit* the data with many points, in effect optimizing parameters of the underlying potentials so that they produce *similar* results for a large number of bound states. In the fit to real data, we have instead a very few lowest-lying bound states, and *solve* for the parameters of trajectories. Implicitly, we demand that the underlying potentials produce the *same* results at those input points. Since the points are the lowest-lying bound states, this corresponds to “aligning” the potentials in the region relevant for the lowest-lying bound states, which can, and should be expected to, lead to different asymptotic values. Since the asymptotic value of the potential is directly related to the threshold of the Regge trajectory (at least in the toy model), this translates into the thresholds for square root and logarithmic trajectories being different.

The difference between the extracted thresholds is thus an indicator of systematic errors. Combining errors in quadrature, we conclude that the threshold for the Pomeron trajectory is (9.4 ± 1.6) GeV.

III. CONCLUSIONS ON GLUEBALL SPECTROSCOPY

As is obvious from Eqs. (7) and (11), the square root form of the trajectory with the parameters fitted to scattering data alone gives the same mass predictions as the fit to both the scattering data and the tensor glueball mass, but with larger errors. The fit to both the scattering data and the mass of the 2^{++} glueball from a lattice may give quite precise predictions for higher excited states, providing the lattice value is close to the true mass of the glueball. Note that our method works very well even for higher excited states. Using the fit, Eq. (11), we obtain the following predictions for excited glueball masses: $M(4^{++}) = 4.21 \pm 0.21$ GeV, $M(6^{++}) = 5.41 \pm 0.28$ GeV, and we obtain $M(2^{++}) = 2.38 \pm 0.12$ GeV, with the same central value obtained from purely scattering Pomeron data.

Based on our calculation we conclude that the threshold for tensor glueballs can be expected in the region no lower than 7–8 GeV and no higher than 11–12 GeV. From the fitted values of the thresholds for various meson multiplets, we know that the thresholds for the same flavors, but different multiplets, vary by less than 20%. We expect the same to be true for glueballs.

Note that the glueball threshold is much larger than what we found for ordinary ($q\bar{q}$) light mesons. This is related to the smaller (local in t , not asymptotic, of course) slope for the Pomeron trajectory but also devolves from our DAMA approach. From this higher value, we infer that a significantly larger number of higher states are available for glueballs than for mesons.

It is also interesting to contemplate what the maximal value of $J = J_{\max}$ may be for the states allowed. We recall from our previous work [1] that the square root trajectory tends to overestimate the growth near the threshold; that is, at any given mass it tends to predict slightly high angular momentum for states approaching the threshold. This was expected from model studies and further confirmed by fits to light meson spectra where sufficient data were available. For

example, for the a_2 trajectory the square root form allowed for a $J=8$ state, whereas we concluded that $J=6$ should actually be the last state on the trajectory.

The glueball trajectory allows for very large values of J_{\max} , possibly as high as 36. The specific value of J_{\max} is obviously subject to a large uncertainty, but our conclusion is firm that the value will be significantly larger than that for ordinary mesons, possibly even larger than that for heavy quarkonia. This raises the paradoxical possibility that high J glueballs may be sufficiently narrow to identify experimentally. (The only other states expected to be available to mix with them would be heavy quarkonia. Such mixing is suppressed to perturbative values by the heavy quark mass.)

Unfortunately, the Pomeron trajectory is the only glueball trajectory for which experimental data are available, and we expect that there are certain exceptional aspects associated with it: As for the light quark-antiquark system, a perturbative analysis shows a strong attraction between two gluons with a threshold at zero. Relativistically, this suggests that the two-particle bound state will develop a negative mass-squared, requiring [15] the formation of a gluonic vacuum condensate (which is known to occur) and a mass gap for the lowest scalar state above the shifted vacuum. The Pomeron trajectory does pass through $J=0$ at a negative mass-squared and there is, of course, no physical state there. If the lowest mass scalar glueball is indeed the scalar state as shifted by the formation of the gluon condensate, it need not appear at the mass expected from standard consideration of the daughter trajectories of the Pomeron.

Such a distortion, however, does not appear to occur [13] for the $f_0(980)$ trajectory in the case of light quarks, where the issues of “four quark” states, as well as mixing (including with the scalar glueball), also arise. However, one does not know if this apparent regularity will hold for the Pomeron trajectory states as well. Therefore, it is also interesting to investigate additional glueball states.

In the absence of other data, we turn to lattice QCD. So far, the spectrum of glueballs has only been calculated in quenched QCD. Of the states listed in Ref. [6], the 0^{-+} at 2.59 ± 0.17 GeV and 2^{-+} at 3.10 ± 0.18 GeV should form a common trajectory with an intercept -3.58 ± 1.48 and threshold $\sqrt{T} = 3.90 \pm 0.91$ GeV. Another trajectory is formed by a 1^{+-} at 2.94 ± 0.17 GeV and a 3^{+-} at 3.55 ± 0.21 GeV. Its intercept is -2.60 ± 1.45 and threshold $\sqrt{T} = 4.87 \pm 1.25$ GeV. Note the large errors of the extracted values. The remaining data from Ref. [6] are ambiguous for our purposes because they can contain admixtures of higher angular momentum states.

The values of thresholds extracted from lattice data are significantly lower than the threshold of the Pomeron trajectory, although, within the large errors, they are consistent with the lower limit of the Pomeron threshold. Moreover, since the thresholds for different trajectories of the same flavors can be expected to differ as much as 20%, the apparent disagreement is not alarming. Unquenched lattice data, therefore, could be very useful for further advancing our understanding of the nature of the Pomeron trajectory, in the absence of further experimental evidence.

IV. FUTURE PROSPECTS

As a prospect for future work, we comment on the possibility of applying our approach to hybrid mesons, which are of current interest to both experiment and theory. In Ref. [6], the authors used the LOBO approximation to calculate spectra of bottomonium as well as bottomoniumlike hybrids. The LOBO approximation was demonstrated to be an efficient and reliable method. However, the potentials used as inputs are generated in quenched lattice QCD, and thus not all of the states predicted may survive in an unquenched theory. Color screening due to light quarks can be expected to become more and more important with the increasing size of the hadron.

Exactly how many of the hybrid states can be reliably extracted from a quenched calculation is unclear. For example, the wave function of the lowest-lying hybrid is found to be larger than that of the lowest-lying quarkonium, but still smaller than the scale where flux tube breakage is expected [6]. There is evidence that survival of the lowest-lying hybrids as well-defined resonances remains conceivable [16].

Unfortunately, implementing the physics of flux tube breaking in lattice QCD is very difficult at present. This is where our phenomenological approach can be of assistance. The key assumption is that because the curvature of the Regge trajectory arises due to the screening and breakage of a flux tube, we can use the same (that is, square root) form of the trajectories as for ordinary mesons.

It is also unfortunate that, at present, only spin-averaged

lattice data are available for the bottomoniumlike hybrids [6]. If the physical states are nearly degenerate, i.e., spin splittings are small, then the spin-averaged data can be used to extract the parameters of the Regge trajectories, and, in particular, the threshold value can be reliable. For example, in pure $q\bar{q}$ mesons, the bottom mass provides a sufficient suppression factor for the subleading splittings, whereas the charm mass is insufficient. In the case of bottomoniumlike hybrids, most possible spin-dependent operators are suppressed by the heavy quark mass. However, there is a contribution due to the angular momentum of the glue that can be expected to be of the same magnitude as the LOBO splittings. This invalidates any conclusions one could draw using our approach based on the leading-order splittings at present. Given more precise lattice data, it would be interesting to compare trajectory parameters of hybrids to those of ordinary mesons and or glueballs.

It should also be worthwhile to examine daughter trajectories using our approach. Conversely to the above, a plethora of relevant experimental evidence is available. A key question here is whether the thresholds for the daughter trajectories are consistent with those found for the parents.

ACKNOWLEDGMENTS

This research is supported by the Department of Energy under Contracts No. W-7405-ENG-36 and DE-FG02-87ER40365.

-
- [1] M. M. Brisudova, L. Burakovsky, and T. Goldman, Phys. Rev. D **61**, 054013 (2000).
- [2] Linear trajectories are, in fact, disfavored by various experimental data. For more details, we refer the reader to discussions in Ref. [1].
- [3] A. I. Bugrij, G. Cohen-Tannoudji, L. L. Jenkovszky, and N. I. Kobylinsky, Fortschr. Phys. **21**, 427 (1973).
- [4] L. Burakovsky, hep-ph/9904322.
- [5] M. M. Brisudová, L. Burakovsky, and T. Goldman, Phys. Lett. B **460**, 1 (1999).
- [6] C. J. Morningstar and M. Peardon, Phys. Rev. D **60**, 034509 (1999); C. Morningstar, nucl-th/0110074.
- [7] D. Q. Liu, J. M. Wu, and Y. Chen, High Energy Phys. Nucl. Phys. **26**, 222 (2002); F. Niedermayer, P. Rufenacht, and U. Wenger, Nucl. Phys. **B597**, 413 (2001); M. J. Teper, hep-lat/9711011; W. J. Lee and D. Weingarten, hep-lat/9805029; H. Chen, J. Sexton, A. Vaccarino, and D. Weingarten, Nucl. Phys. B (Proc. Suppl.) **34**, 357 (1994); UKQCD Collaboration, G. S. Bali, K. Schilling, A. Hulsebos, A. C. Irving, C. Michael, and P. W. Stephenson, Phys. Lett. B **309**, 378 (1993); A. Hart and M. Teper, Phys. Rev. D **65**, 034502 (2002).
- [8] G. Veneziano, Phys. Rep. **9**, 199 (1974).
- [9] L. L. Jenkovszky, Riv. Nuovo Cimento **10**, 1 (1987).
- [10] A. A. Trushevsky, Ukr. Fiz. Zh. (Russ. Ed.) **22**, 353 (1977).
- [11] D. Crewther and G. C. Joshi, Phys. Rev. D **9**, 1446 (1974).
- [12] ZEUS Collaboration, J. Breitweg *et al.*, Eur. Phys. J. C **14**, 213 (2000); see also A. Levy, hep-ph/0008130.
- [13] C. E. Allgower and D. C. Peaslee, Phys. Lett. B **513**, 273 (2001).
- [14] K. D. Born *et al.*, Phys. Rev. D **40**, 1653 (1989).
- [15] Y. Nambu and G. Jona-Lasinio, Phys. Rev. **123**, 345 (1961); **124**, 246 (1961).
- [16] K. J. Juge, J. Kuti, and C. J. Morningstar, Phys. Rev. Lett. **82**, 4400 (1999).